Geophysical Research Letters

RESEARCH LETTER
10.1029/2022GL102324

The Mini Induced Magnetospheres at Mars

E. Dubinin[1], M. Fraenz[1], M. Pätzold[2], S. Tellmann[2], G. DiBraccio[3], and J. McFadden[4]

[1]Max-Planck-Institute for Solar System Research, Göttingen, Germany, [2]Rheinisches Institut fuer Umweltforschung, Abteilung Planetforschung, Cologne, Germany, [3]NASA Goddard Space Flight Center, Greenbelt, MD, USA, [4]Space Sciences Laboratory, University of California Berkeley, Berkeley, CA, USA

Key Points:

- Oxygen ions extracted from the Martian ionosphere interact with shocked solar wind in the magnetosheath
- When the ion densities of both plasmas become comparable the mini induced magnetospheres are built
- These Magnetospheres possess all typical features of the classical induced magnetospheres

Correspondence to:
E. Dubinin,
dubinin@mps.mpg.de

Citation:
Dubinin, E., Fraenz, M., Pätzold, M., Tellmann, S., DiBraccio, G., & McFadden, J. (2023). The mini induced magnetospheres at Mars. *Geophysical Research Letters*, *50*, e2022GL102324. https://doi.org/10.1029/2022GL102324

Received 30 NOV 2022
Accepted 30 JAN 2023

Author Contributions:
Conceptualization: E. Dubinin
Data curation: J. McFadden
Formal analysis: J. McFadden
Investigation: E. Dubinin, M. Fraenz, M. Pätzold, G. DiBraccio
Methodology: M. Pätzold, S. Tellmann, G. DiBraccio
Resources: M. Pätzold, S. Tellmann
Software: M. Fraenz
Validation: S. Tellmann, G. DiBraccio, J. McFadden
Writing – original draft: E. Dubinin

Abstract We report on observations made by the Mars Atmosphere and Volatile EvolutioN spacecraft at Mars, in the region of the ion plume. We observe that in some cases, when the number density of oxygen ions is comparable to the density of the solar wind protons interaction between both plasmas leads to formation in the magnetosheath of mini induced magnetospheres possessing all typical features of induced magnetospheres typically observed at Mars or Venus: a pileup of the magnetic field at the head of the ion cloud, magnetospheric cavity, partially void of solar wind protons, draping of the interplanetary magnetic field around the mini obstacle, formation of a magnetic tail with a current sheet, in which protons are accelerated by the magnetic field tensions. These new observations may shed a light on the mechanism of formation of induced magnetospheres.

Plain Language Summary There is a class of the induced planetary magnetospheres when the absence of intrinsic magnetic field allows a direct interaction of solar wind with planetary atmospheres/ionospheres. We have shown the existence of mini-induced magnetospheres at Mars. When the density of the extracted from the ionosphere oxygen ions becomes comparable with the proton density in solar wind mini-induced magnetospheres with all typical features of the planetary induced magnetospheres arise.

1. Introduction

The absence of a global magnetic field at Mars leads to a nearly direct interaction of solar wind with the ionosphere and to the formation of an induced magnetosphere where the interplanetary magnetic field (IMF) drapes around the ionospheric obstacle. On the other hand, existence of strong localized crustal magnetic fields (Acuna et al., 1999; Connerney et al., 2005) adds features typical for planets with a global intrinsic magnetic field. As a result, the Martian magnetosphere contains elements of induced and intrinsic origin (see e.g., Brain, 2021; E. Dubinin et al., 2011, 2020; Halekas et al., 2021; Nagy et al., 2004). There are many planets, satellites and comets possessing induced magnetospheres—Venus (Luhmann, 1995; Russell and Vaisberg, 1983), Titan (Bertucci et al., 2008; Ness et al., 1982), Pluto (McComas et al., 2016), comets (Gombosi, 2015; Nilsson et al., 2021). Artificial induced magnetospheres were even created in plasma laboratories and in space (Haerendel et al., 1986; Podgorny et al., 1979). In induced magnetospheres solar wind dynamic pressure is converted to magnetic pressure by compressing the IMF which drapes around the ionospheric obstacle. The compressed field forms a magnetic barrier and a magnetospheric cavity almost void of solar wind. The draped IMF lines in the wake form a long magnetic tail on the night side (E. Dubinin and Fraenz, 2015). The well-organized structure of the induced magnetic tail consists of two lobes with oppositely directed magnetic field lines, separated by a plasma sheet. Draping of the IMF lines around Mars is asymmetric with respect to the direction of the motional electric field with a shift of the position of the upstream magnetic field pileup toward the $-V \times B$ side (E^+ hemisphere) (E. Dubinin et al., 2019; Modolo et al., 2016). An important feature of the induced magnetosphere at Mars is the extraction of the ionospheric oxygen ions in the E^+ hemisphere where the motional electric field $-V_{sw} \times B$ points outward from the planet. The energy of extracted ions increases with distance from Mars (E. Dubinin, Lundin, et al., 2006) and they form an ion plume that is one of escape channels for ion loss (Dong et al., 2015). The incursion of oxygen ions into the Martian magnetosheath and undisturbed solar wind lead to a direct interaction of both plasmas.

In this study we analyzed several cases of such an interaction between plume ions and shocked solar wind in the Martian magnetosheath. The observations were made by the Mars Atmosphere and Volatile EvolutioN (MAVEN) spacecraft in the ion plume. MAVEN arrived at Mars in September 2014 to study the processes in the upper atmosphere/ionosphere and its interaction with the solar wind (Jakosky et al., 2015) and was inserted into

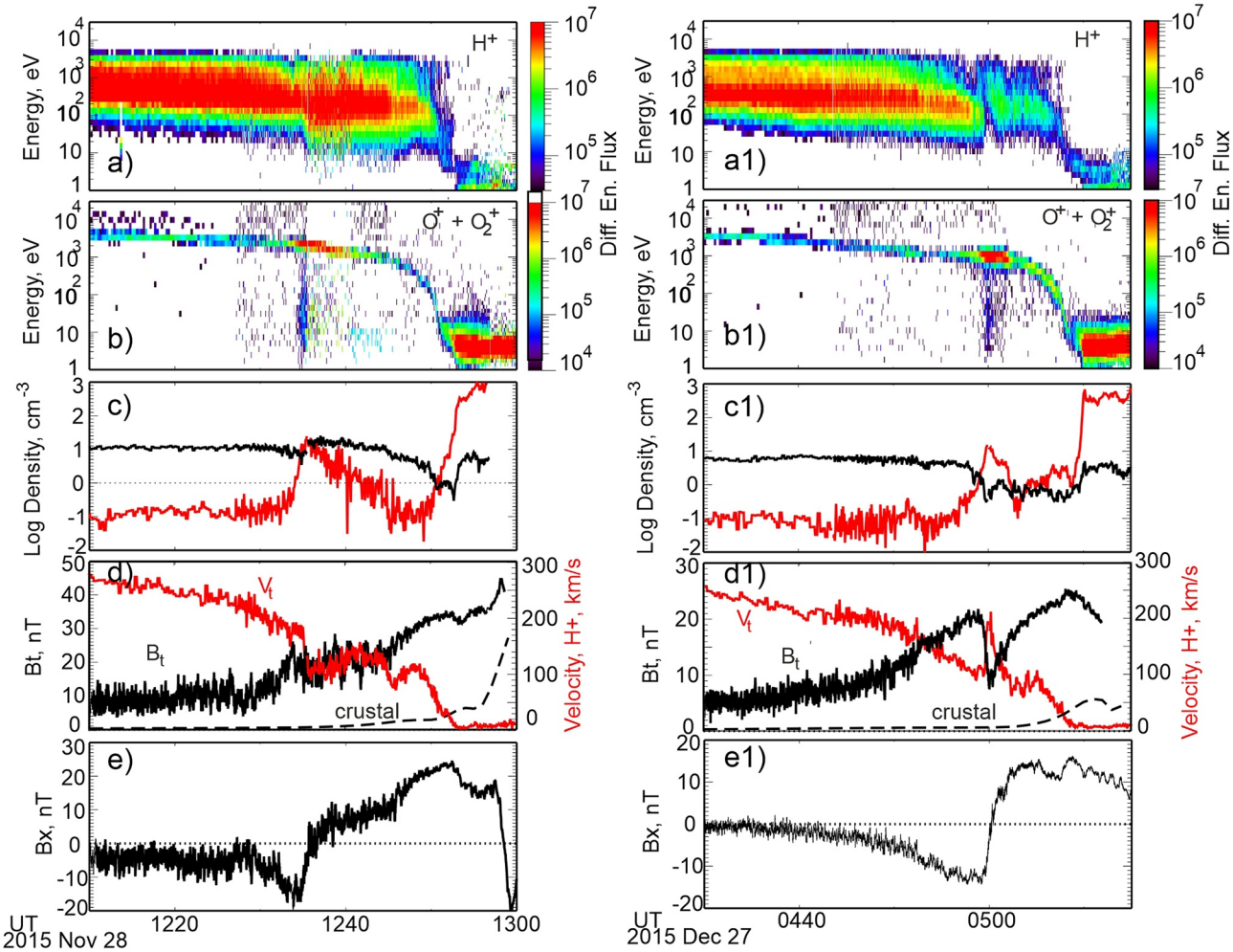

Figure 1. Particle and field data from Mars Atmosphere and Volatile EvolutioN measurements on two orbits. From top to bottom: spectrograms of differential energy fluxes of protons, oxygen ions (O^+ and O_2^+); number density of protons (black curves) and oxygen ions (red curves); the magnetic field magnitude (black curve) and the speed of protons (red curves); B_x-component of the magnetic field.

an elliptical orbit with periapsis and apoapsis of 150 and 6,200 km, respectively, and with a period of 4.5 hr. In this paper, we discuss observations made by the magnetometer (Connerney et al., 2015) and the Supra-Thermal And Thermal Ion Composition (STATIC) instrument (McFadden et al., 2015). The STATIC measurements allow a retrieval of the velocity distribution functions of H^+, He^{++}, O^+, O_2^+, CO_2^+ ions. From this time series we calculate density, velocity, thermal pressure and temperature for the different sorts of ions (Fraenz et al., 2006). Because of angular coverage limitations of the STATIC sensor, we only estimate the three diagonal terms of tensor of ion pressure and calculate pressure as $P = \Sigma P_{ii}/3$.

We find that when the local density of the extracted oxygen ions is comparable or even exceeds the local solar wind proton number density features typical for global induced magnetospheres can be observed around the local oxygen clouds.

2. Observations

Figure 1 shows examples of MAVEN particle and field data from the measurements made in the region of the ion plume. Upper panels (a) and (a1) depict the spectrograms of the proton fluxes. MAVEN is moving in the magnetosheath approaching the magnetosphere boundary clearly identified from a drop of the proton fluxes. Panels (b) and (b1) present the energy differential fluxes of oxygen (O^+ and O_2^+) ions. Ions in the plume extracted from the Martian ionosphere and gaining energy in the motional electric field are clearly seen. What sets the observation

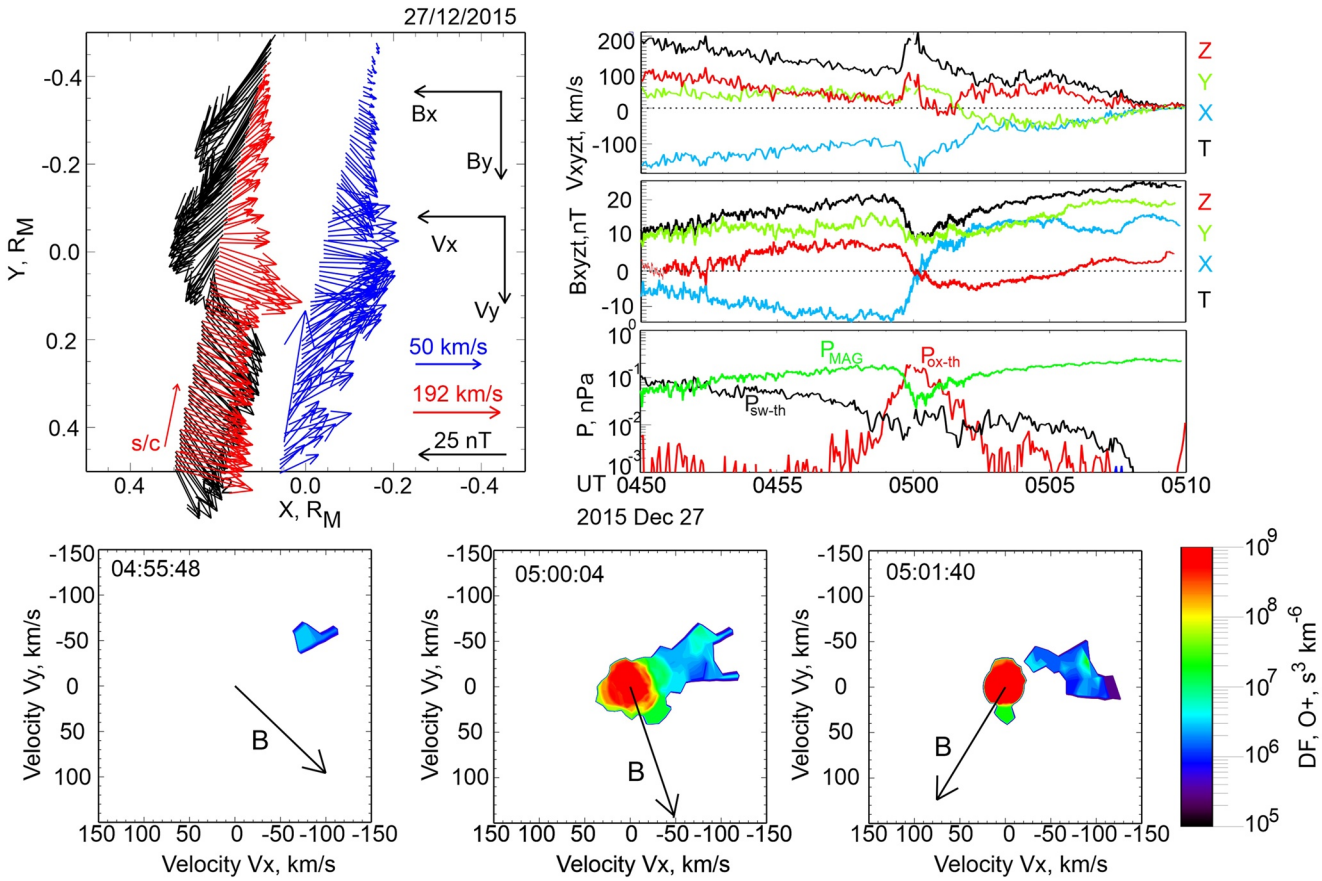

Figure 2. (upper panels) (right) Three components of the proton velocity and the total speed; three components of the magnetic field and the total value; the magnetic field pressure (green), thermal pressure of protons (black) and thermal pressure of oxygen ions (red) across the current sheet in the mini induced magnetosphere. (left) projections of the field vectors (black), vectors of the proton velocity (red) and oxygen ions (blue) onto XY-Mars Solar Orbital plane. Lower row shows the examples of the distribution functions of oxygen ions.

apart from a typical ion plume is a sudden appearance of ion fluxes with a broad energy distribution. The oxygen ion density in these narrow plasma streams/clouds (red curves in panels c and c1) strongly increases reaching the density of the shocked solar wind protons (black curves in panels c and c1). The impinging of the proton flow with the oxygen cloud is accompanied by strong variations in the magnetic field and the proton speed (panels d and d1). In the event on 28 November 2015, the magnetic field strength increases while on 27 December 2015 it sharply decreases. In contrast, the proton bulk speed in these events decreases (increases). The B_x component of the magnetic field in both cases changes sign (panels e and e1) pointing to a draping of the magnetic field lines around the oxygen ion cloud/stream. This is reminiscent of the behavior of particles and fields when an induced magnetosphere is formed. The crossing by MAVEN of such a mini induced magnetosphere on 28 November corresponds to a typical crossing at the dayside with a pileup of the magnetic field. The data obtained on 27 December well match to a typical crossing in the tail where a plasma jet is formed under action of the magnetic field stresses.

The upper left panel in Figure 2 shows the projections of the magnetic field (black arrows) onto the XY-Mars Solar Orbital plane during crossing of the ion stream/cloud on 27 December. Red arrows present the projections of the proton velocity. Blue arrows on a shifted trajectory depict the projections of the velocity of O^+ ions. Draping of the IMF around the oxygen stream/cloud and proton acceleration in the settled current sheet are observed. We also observe a slight deflection of the magnetosheath plasma around this small obstacle. In contrast, oxygen ions flow into the formed mini-magnetosphere. The lower row shows examples of the projections of the distribution function of oxygen ions in the ion plume and in the oxygen cloud. It is observed that ions in the cloud have a trend of streaming in the same direction with ions in the plume and the magnetosheath flow although with lower velocities. The upper right panel depicts from top to bottom the proton velocity components and its total value,

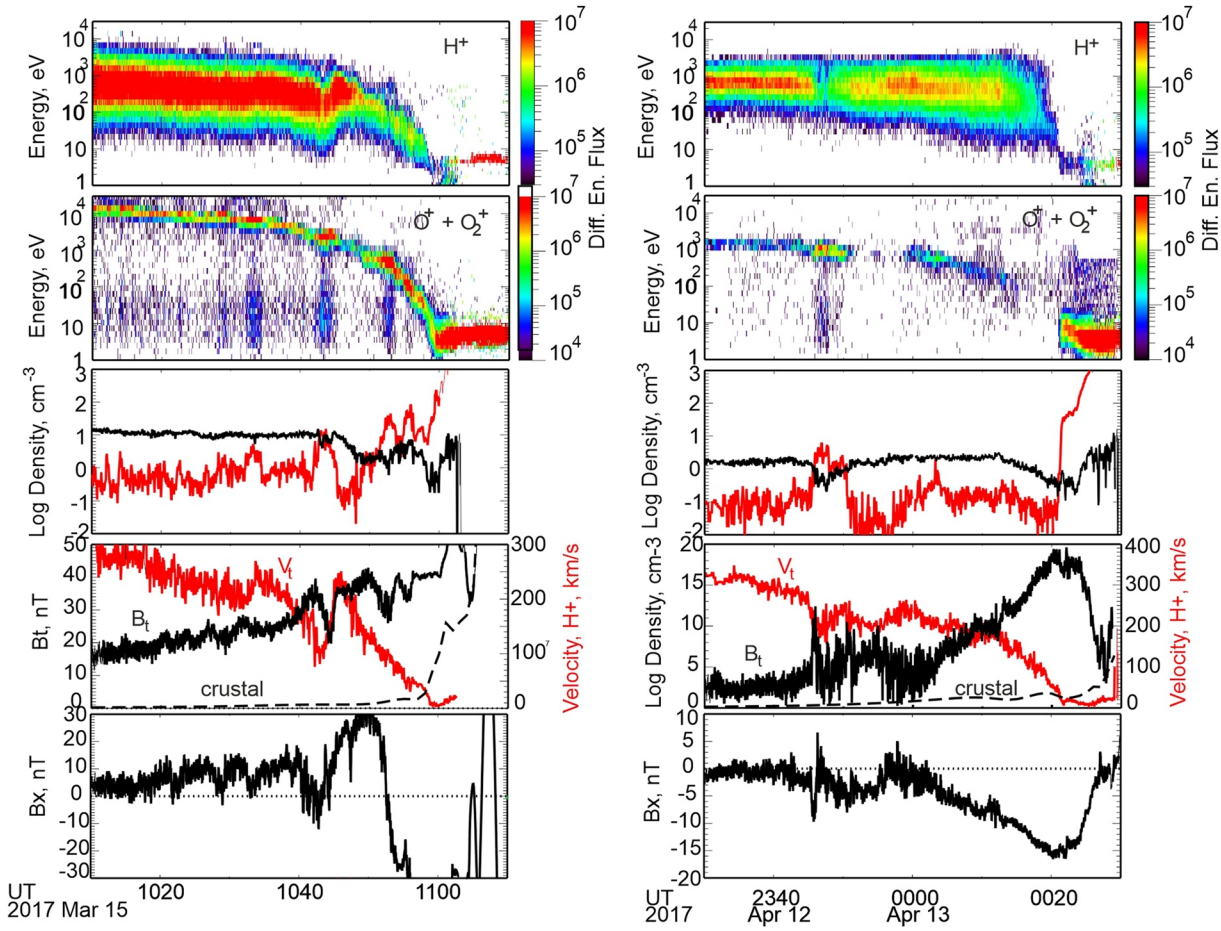

Figure 3. Same as for Figure 1. The bottom panels show the magnetic field pressure (green), thermal pressure of protons (black), thermal pressure of oxygen ions (red) and the dynamic shocked solar wind pressure in the reference frame of the oxygen cloud.

the components of the magnetic field and different pressure terms (thermal pressure was estimated as an average of three diagonal terms in pressure tensor). The gain in proton speed in the current sheet is about ∼120 km/s which might be compared with the Alfven speed (∼160 km/s) in the magnetosheath plasma. A balance between the magnetic pressure and the thermal pressure of oxygen ions observed at ∼05:00 UT indicates a dynamic equilibrium. It is worth noting that the dynamic pressure of the proton flow in the reference frame of the ion cloud is small.

Figure 3a shows a more complicated case when we observe three oxygen streams/clouds in the magnetosheath and in the adjacent boundary layer. In the event, at ∼10:34 the proton speed increases although the spacecraft does not completely cross the current sheet. In the event centered at ∼10:43 the proton velocity and the proton number density decrease. This indicates entry to the head part of the mini induced magnetosphere. The third event occurs very close to the boundary of the Martian magnetosphere (∼10:52:30). The crossing is defined by a sharp reversal of the magnetic field, but without a noticeable change in the proton speed. Note, that the number density of oxygen ions in this case is about 40 times higher than the density of protons. Figure 3b depicts an example with a more pronounced cavity (at ∼23:47) for the streaming shocked solar wind crossing the mini induced magnetosphere. The proton density in the sheath drops almost by factor eight and the oxygen ions completely dominate the plasma. The drop is accompanied by a sharp decrease in the proton speed and a narrow jump of the magnetic field strength B_t that can be interpreted as a magnetic barrier in front of the proton cavity. The bottom panels in Figure 3 show the pressure terms. For events observed on March 15 the solar wind protons and oxygen ions move with approximately the same speed and therefore in the reference frame of the oxygen cloud the dynamic pressure of the sheath plasma is small. A pressure balance in the event at ∼10:43 is ensured between the magnetic pressure $B^2/8\pi$ and the thermal pressure of the ion oxygen cloud nkT_i. On 12 April,

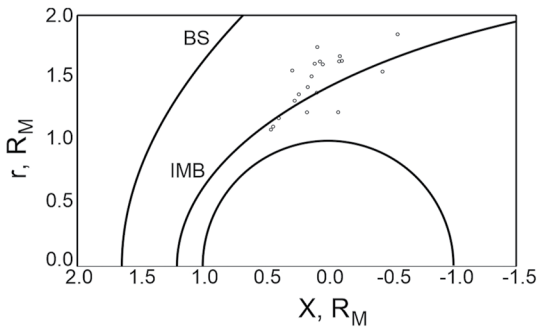

Figure 4. Location of mini induced magnetospheres in cylindrical coordinates. Nominal positions of the bow shock and the induced magnetosphere boundary (Dubinin, Fraenz, et al., 2006; Vignes et al., 2000) are also shown.

contribution of the dynamic pressure becomes important and the pressure balance is achieved in two steps: $\rho\Delta V^2 \sim B^2/8\pi \sim nkT_i$.

We have found about 20 similar structures in 4 years of observations by the MAVEN spacecraft. Figure 4 shows their positions in cylindrical coordinates. Mini induced magnetospheres were detected in the sheath, usually rather close to the nominal position of the induced magnetospheric boundary. Note that during events inside the nominal position the real boundary was observed at lower altitudes.

3. Discussion and Conclusions

3.1. Size and Shape of Induced Mini-Magnetosphere

The size of the induced mini-magnetospheres can be roughly estimated from the time interval of the crossing and the ion oxygen velocity which is usually higher than the spacecraft speed. The size varies from several hundreds to several thousand km. It is not clear whether such structures are detached from the ionosphere or attached. Figure 5 shows two sketches of the Martian space with a planetary magnetosphere with embedded mini intrinsic magnetospheres generated by the existence of crustal magnetic fields and mini induced magnetospheres during strong oxygen ion injection into the ion plume in the magnetosheath. In one case, the mini magnetospheres are detached structures while in another case, mini magnetospheres are formed around moving and folding plasma rays resembling plasma clumps in the Active Magnetospheric Particle Tracer Explorer Ba release (Valenzuela et al., 1986) or ray structures at comets (Bonev & Jokers, 1994; Sauer & Dubinin, 1999). Extension of the draping field lines in the region of ion plume to the nightside of the Martian magnetosphere will produce extra structures in the tail lobes and the current sheet.

3.2. Pressure Balance and Forces

We observe different pressure balance processes on the dayside of the mini induced magnetospheres. In some cases shocked solar wind and the ion stream/cloud move with approximately the same speed and in such quasi-static configurations the thermal pressure in the ion stream is balanced by increased magnetic pressure. In other cases protons move much faster and the dynamic pressure exerted on the ion stream is balanced by pressure of the piled up magnetic field which in turn is balanced by the thermal plasma pressure in ion streams. Forces playing in such interaction depend on the relative values of the spatial scale δ of the field enhancement

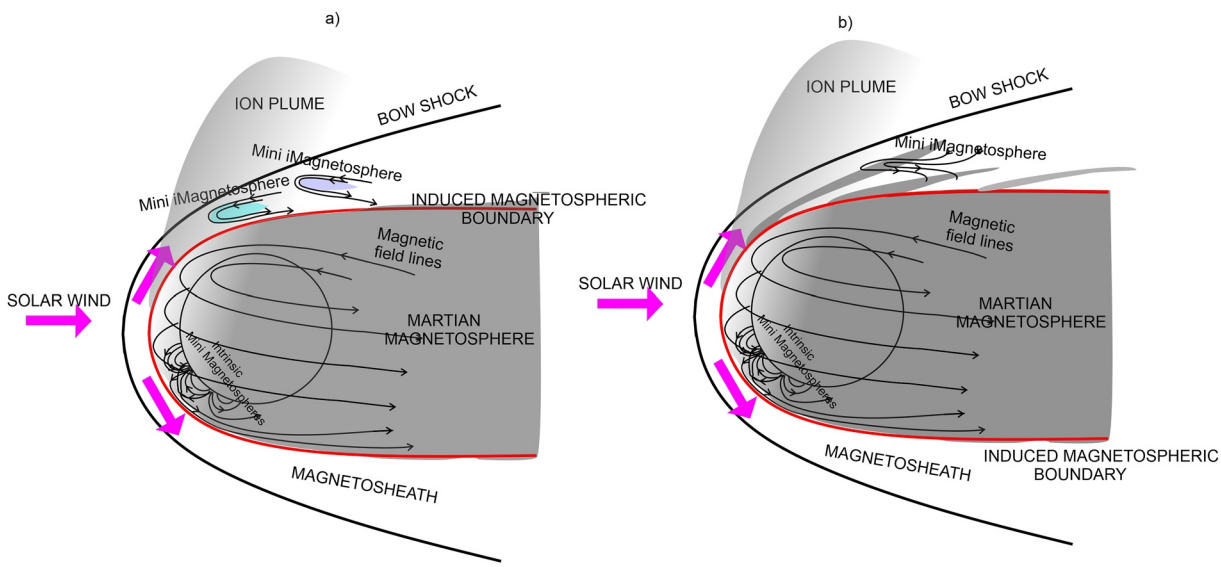

Figure 5. Sketches of the Martian space containing a global magnetosphere and mini intrinsic and mini induced magnetospheres.

in the magnetic barrier and the ion skin length c/Ω_i. The ion skin length is typically 100–300 km. It is more difficult to estimate the characteristic scale because the different elements of clouds move with different velocities (see e.g., Figure 2). In some events, as for example, in 12 April 2017 it can vary from ~200–1,000 km and therefore might be comparable to the ion skin length (100–150 km). For such cases the real force which decelerates and deflects the impinging shocked solar wind protons is the Hall electric field directed outward from the barrier, perpendicular to the magnetic field, and balancing the dynamic pressure. The drift of electrons in E×B fields generates a current responsible for pileup of the magnetic field. At the boundary between the piled up magnetic field and ion cloud the Hall electric field is pointed in the opposite, inward direction and balances the gradient of the thermal pressure in ion stream. For the events when $\delta \gg c/\Omega_i$, the current is maintained by the diamagnetic drift of ions. For accurate determination of the characteristic scale we have to distinguish the spatial and temporal variations. It can be done, for example, in the future ESCAPADE project with two spacecraft.

3.3. Ion Composition Boundary

An interesting feature is that mini-magnetospheres are formed when the ion density in the streams/clouds reaches the density of the flowing protons in the shocked solar wind. This again raises the question about the role of the ion composition boundary (ICB) in formation of induced magnetospheres. This term was introduced in Breus et al. (1991), Sauer and Dubinin (2000), and Sauer et al. (1994, 1995) to describe the boundary of the Martian magnetosphere. Halekas et al. (2018) have found that the compositional transition at Mars on average lies at or below the altitude where pressure balance between shocked solar wind and the magnetic barrier is maintained, and is not sensitive to variations in solar zenith angle and solar wind parameters. The existence of such a boundary might be related to the Lorentz force $\sim n_p n_h/n_e(V_p - V_h) \times B$ in the momentum equation for protons in the multi-ion fluid magnetohydrodynamics equations (Chapman & Dunlop, 1986; E. Dubinin et al., 2011; Harold & Hassam, 1994; Halekas et al., 2018; Sauer et al., 1994) which describes the mass-loading process. For $n_h \ll n_p$ this force is small while at $n_p \sim n_h$ the force can strongly deflect the proton flow. Another alternative is that the ICB corresponds to a critical point in plasma consisting of several ion species. At this point a regular plasma flow is broken and a new flow configuration can be formed (E. M. Dubinin, Sauer, & McKenzie, 2006). In any case, the existence of the ICB might be a general feature of the formation of induced magnetospheres and requires further analysis.

In conclusion, it is shown that during the enhanced oxygen ion extraction from the Martian ionosphere into the ion plume in the magnetosheath, interaction of the shocked solar wind with localized ionospheric plasmas leads to formation of mini induced magnetospheres. These mini magnetospheres have all characteristic properties of planetary induced magnetospheres (draping of the IMF around mini obstacles, magnetic barrier, magnetospheric cavity for solar wind protons, tail with a current sheet).

Data Availability Statement

MAVEN data are publicly available through the Planetary Plasma Interactions Node of the Planetary Data System (https://pds-ppi.igpp.ucla.edu/mission/MAVEN/MAVEN/MAG) and (https://pds-ppi.igpp.ucla.edu/mission/MAVEN/MAVEN/STATIC).

Acknowledgments
The MAVEN project is supported by NASA through the Mars Exploration Program. Authors ED, MP, ST wish to acknowledge support from DFG for supporting this work by Grants TE 664/4-1 and PA 525/25-1. Open Access funding enabled and organized by Projekt DEAL.

References

Acuña, M., Connerney, J. E. P., Ness, N. F., Lin, R. O., Mitchell, D., Carlson, C. W., et al. (1999). Global distribution of crustal magnetism discovered by Mars Global Surveyor MAG/ER experiment. *Science*, *284*(5415), 790–793. https://doi.org/10.1126/science.284.5415.790

Bertucci, C., Achilleos, N., Dougherty, M. K., Modolo, R., Coates, A. J., Szego, K., et al. (2008). The magnetic memory of Titan's ionized atmosphere. *Science*, *321*(5895), 1475–1478. https://doi.org/10.1126/science.1159780

Bonev, T., & Jokers, K. (1994). H_2O^+ ions in the inner plasma tail of comet Austin 1990 V. *Icarus*, *107*(2), 335–357. https://doi.org/10.1006/icar.1994.1028

Brain, D. (2021). Induced magnetospheres, atmospheric escape. In R. Maggiolo, N. André, H. Hasegawa, D. Welling, L. Paxton, Y. Zhang, et al. (Eds.), *Magnetospheres in the solar system, geophysical monograph series*. https://doi.org/10.1002/9781119815624.ch28

Breus, T., Krymskii, A., Dubinin, E., Yeroshenko, E., Mitnitskii, V., Pissarenko, N., et al. (1991). Solar wind interaction with Mars, Phobos-2 data. *Cosmic Research*, 741–753.

Chapman, S. C., & Dunlop, M. W. (1986). Ordering of momentum transfer along V×B in the AMPTE solar wind releases. *Journal of Geophysical Research*, *91*(A7), 8051–8055. https://doi.org/10.1029/ja091ia07p08051

Connerney, J. E. P., Acuna, M. H., Ness, N. F., Kletetschka, G., Mitchell, D. L., Lin, R. P., & Reme, H. (2005). Tectonic implications of Mars crustal magnetism. *Proceedings of the National Academy of Sciences of the United States of America*, *102*(42), 14970–14975. https://doi.org/10.1073/pnas.0507469102

Connerney, J. E. P., Espley, J., Lawton, P., Murphy, S., Odom, J., Olivers, R., & Sheppard, D. (2015). The MAVEN magnetic field investigation. *Space Science Reviews*, *195*(1–4), 257–291. https://doi.org/10.1007/s11214-015-0169-4

Dong, Y., Fang, X., Brain, D. A., McFadden, J. P., Halekas, J. S., Connerney, J. E., et al. (2015). Strong plume fluxes at Mars observed by MAVEN: An important planetary ion escape channel. *Geophysical Research Letters*, *42*(21), 8942–8950. https://doi.org/10.1002/2015GL065346

Dubinin, E., Fraenz, M., Fedorov, A., Lundin, R., Edberg, N., Duru, F., & Vaisberg, O. (2011). Ion energization and escape on Mars and Venus. *Space Science Reviews*, *162*(1–4), 173–211. https://doi.org/10.1007/978-1-4614-3290-6-6

Dubinin, E., & Fraenz, M. (2015). Magnetotails of Mars and Venus. In A. Keiling, C. M. Jackman, & P. A. Delamere (Eds.), *Magnetotails in the solar system* (pp. 43–59). John Wiley & Sons, Inc. https://doi.org/10.1002/9781118842324.ch3

Dubinin, E., Fraenz, M., Modolo, R., Pätzold, M., Tellmann, S., Vaisberg, O., et al. (2021). Induced magnetic fields and plasma motions in the inner part of the Martian magnetosphere. *Journal of Geophysical Research: Space Physics*, *126*, e2021JA029542. https://doi.org/10.1029/2021JA029542

Dubinin, E., Fraenz, M., Woch, J., Roussos, E., Barabash, S., Lundin, R., et al. (2006). Plasma morphology at Mars: ASPERA-3 observations. *Space Science Reviews*, *126*(1–4), 209–238. https://doi.org/10.1007/s11214-006-9039-4

Dubinin, E., Luhmann, J., & Slavin, J. (2020). Solar wind and terrestrial planets. In *Oxford research encyclopedia of planetary science*. Oxford University Press. https://doi.org/10.1093/acrefore/9780190647926.013.184

Dubinin, E., Lundin, R., Fraenz, M., Woch, J., Barabash, S., Fedorov, A., et al. (2006). Electric Fields within the Martian magnetosphere and ion extraction. ASPERA observations. *Icarus*, *182*(2), 337–342. https://doi.org/10.1016/j.icarus.2005.05.022

Dubinin, E., Modolo, R., Fraenz, M., Pätzold, M., Woch, J., Chai, L., et al. (2019). The induced magnetosphere of Mars: Asymmetrical topology of the magnetic field lines. *Geophysical Research Letters*, *46*(22), 12722–12730. https://doi.org/10.1029/2019GL084387

Dubinin, E. M., Sauer, K., & McKenzie, J. F. (2006). Nonlinear 1-D stationary flows in multi-ion plasmas? Sonic and critical loci? Solitary and "oscillatory waves". *Annales de Geophysique*, *24*(11), 3041–3057. https://doi.org/10.5194/angeo-24-3041-2006

Fraenz, M., Dubinin, E., Roussos, E., Woch, J., Winningham, J. D., Frahm, R., et al. (2006). Plasma moments in the environment of Mars, Mars Express ASPERA-3 observations. *Space Science Reviews*, *126*(1–4), 165–207. https://doi.org/10.1007/s11214-006-9115-9

Gombosi, T. (2015). Physics of cometary magnetospheres. In A. Keiling, C. Jackman, & P. Delamere (Eds.), *Magnetotails in the solar system, geophysical monograph series*. https://doi.org/10.1002/9781118842324.ch10

Haerendel, G., Paschmann, G., Baumjohann, W., & Carlson, C. W. (1986). Dynamics of the AMPTE artificial comet. *Nature*, *320*(6064), 720–723. https://doi.org/10.1038/320720a0

Halekas, J. S., Luhmann, J. G., Dubinin, E., & Ma, Y. (2021). Induced magnetospheres: Mars. In B.R. Maggiolo, N. Andre, H. Hasegawa, D. Welling, Y. Zhang, et al. (Eds.), *magnetospheres in solar system, geophysics monograph series*. https://doi.org/10.1002/9781119815624.ch25

Halekas, J. S., McFadden, J. P., Brain, D. A., Luhmann, J. G., DiBraccio, G. A., Connerney, J. E. P., et al. (2018). Structure and variability of the Martian ion composition boundary layer. *Journal of Geophysical Research: Space Physics*, *123*(10), 8439–8458. https://doi.org/10.1029/2018JA025866

Harold, J. B., & Hassam, A. B. (1994). Two ion fluid numerical investigations of solar wind gas releases. *Journal of Geophysical Research*, *99*(A10), 19325–19340. https://doi.org/10.1029/94ja00790

Jakosky, B. M., Lin, R. P., Grebowsky, J. M., Luhmann, J. G., Mitchell, D. F., Beutelschies, G., et al. (2015). The Mars atmosphere and volatile evolution (MAVEN) mission. *Space Science Reviews*, *195*(1–4), 3–48. https://doi.org/10.1007/s11214-015-0139-x

Luhmann, J. G. (1995). In M. G. Kivelson & C. T. Russell (Eds.), *Introduction to space physics*. Cambridge University Press.

McComas, D. J., Elliott, H. A., Weidner, S., Valek, P., Zirnstein, E. J., Bagenal, F., et al. (2016). Pluto's interaction with the solar wind. *Journal of Geophysical Research: Space Physics*, *121*(5), 4232–4246. https://doi.org/10.1002/2016JA022599

McFadden, J. P., Kortmann, O., Curtis, D., Dalton, G., Johnson, G., Abiad, R., et al. (2015). MAVEN SupraThermal and thermal ion composition (STATIC) instrument. *Space Science Reviews*, *195*(1–4), 199–256. https://doi.org/10.1007/s11214-015-175-6

Modolo, R., Hess, S., Mancini, M., Leblanc, F., Chaufray, J. Y., Brain, D., et al. (2016). Mars-solarwind interaction: LatHyS, an improved parallel 3-D multispecies hybrid model. *Journal of Geophysical Research: Space Physics*, *121*(7), 6378–6399. https://doi.org/10.1002/2015JA022324

Nagy, A. F., Winterhalter, K., Sauer, K., Cravens, T., Brecht, S., Mazelle, C., et al. (2004). The plasma environment of Mars. *Space Science Reviews*, *11*(1–2), 38–114. https://doi.org/10.1023/b:spac.0000032718.47512.92

Ness, N. F., Acuña, M. H., Behannon, K. W., & Neubauer, F. M. (1982). The induced magnetosphere of Titan. *Journal of Geophysical Research*, *87*(A3), 1369–1381. https://doi.org/10.1029/ja087ia03p01369

Nilsson, H., Behar, E., Burch, J., Carr, M., Eriksson, I., Glassmeier, K.-H., et al. (2021). Birth of a magnetosphere. In R. Maggiolo, N. André, H. Hasegawa, D. Welling, L. Paxton, & Y. Zhang (Eds.), *Magnetospheres in the solar system* (Vol. 259, pp. 427–439). Wiley-American Geophysical Union. https://doi.org/10.1002/9781119815624.ch27

Podgorny, I., Dubinin, E., Potanin, Y., & Shkolnikov a, S. (1979). Simulation of cometary magnetic tails. *Astrophysics and Space Science*, *61*(2), 369–374. https://doi.org/10.1007/bf00640538

Russell, C. T., & Vaisberg, O. (1983). Interaction of the solar wind with Venus. In D. M. Hunton, L. Colin, T. M. Donahue, & V. I. Moroz (Eds.), *Venus* (pp. 873–940). University of Arizona Press.

Sauer, K., Bogdanov, A., & Baumgärtel, K. (1994). Evidence of an ion composition boundary (protonopause) in bi-ion fluid simulations of solar wind mass loading. *Geophysical Research Letters*, *21*(20), 153–158. https://doi.org/10.1029/94gl01691

Sauer, K., Bogdanov, A., & Baumgärtel, K. (1995). The protonopause—An ion composition boundary in the magnetosheath of comets, Venus and Mars. *Advances in Space Research*, *16*(4), 2255–2258. https://doi.org/10.1016/0273-1177(95)00223-2

Sauer, K., & Dubinin, E. (1999). Cometosheath structures and tail rays: Outcome of bi-ion fluid simulations. *Earth, Moon, and Planets*, *77*(3), 271–278. https://doi.org/10.1023/a:1006241906247

Sauer, K., & Dubinin, E. (2000). The nature of the Martian 'obstacle boundary'. *Advances in Space Research*, *26*(10), 1633–1637. https://doi.org/10.1016/s0273-1177(00)00109-5

Valenzuela, A., Haerendel, G., Foeppl, H., Melzner, F., Neuss, H., Rieger, E., et al. (1986). The AMPTE artificial comet experiments. *Nature*, *320*(6064), 700–703. https://doi.org/10.1038/320700a0

Vignes, D., Mazelle, C., Rme, H., Acuña, M. H., Connerney, J. E. P., Lin, R. P., et al. (2000). The solar wind interaction with Mars: Locations and shapes of the bow shock and the magnetic pile-up boundary from the observations of the MAG/ER Experiment onboard Mars Global Surveyor. *Geophysical Research Letters*, *27*(1), 49–52. https://doi.org/10.1029/1999GL010703